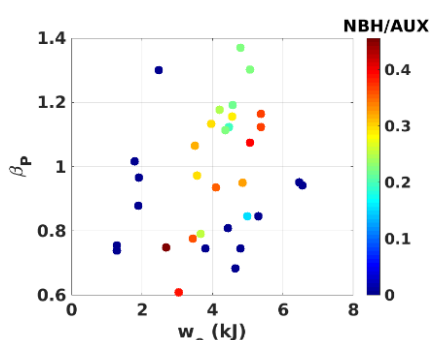


## Nonlinear contribution of neutral beam injection in TCV EC-heated advanced tokamak scenarios

M. Vallar<sup>1</sup>, M. Agostini<sup>1</sup>, T. Bolzonella<sup>1</sup>, S. Coda<sup>2</sup>, J. Garcia<sup>3</sup>, B. Geiger<sup>4</sup>, G. Giruzzi<sup>3</sup>, T. Goodman<sup>2</sup>, M. Gorelenkova<sup>5</sup>, A.N. Karpushov<sup>2</sup>, T. Kurki-Suonio<sup>6</sup>, C. Piron<sup>1</sup>, L. Pigatto<sup>1</sup>, O. Sauter<sup>2</sup>, N. Vianello<sup>1</sup>, P. Vincenzi<sup>1</sup>, M. Yoshida<sup>7</sup> the TCV team and the MST1 team<sup>♦</sup>

1. *Consorzio RFX, Corso Stati Uniti 4, 35127 Padova, Italy*
2. *École Polytechnique Fédérale de Lausanne (EPFL), Swiss Plasma Center (SPC), CH-1015 Lausanne, Switzerland*
3. *CEA, IRFM, 13108 Saint-Paul-lez-Durance, France*
4. *Max Planck Institute for Plasma Physics, Garching, Germany*
5. *Princeton Plasma Physics Laboratory, Princeton University*
6. *Aalto University, P.O. Box 14100, FI-00076 AALTO, Finland*
7. *National Institutes for Quantum and Radiological Science and Technology, Naka, Ibaraki 311-0193, Japan*

**Introduction** - TCV (Tokamak à Configuration Variable) is a tokamak device capable of many different plasma shapes, equipped with a flexible Electron Cyclotron (EC) system and since 2016 with a heating Neutral Beam (NB) injector [1]. The EC system incorporates two subsystems: X2 (second harmonic) used for electron heating up to cutoff density  $4.2 \times 10^{19} \text{ m}^{-3}$  with efficient current drive; X3 extends the density range for EC heating up to higher density



**Figure 1** Poloidal beta vs plasma energy content, with varying NB injected power

$11.2 \times 10^{19} \text{ m}^{-3}$  (cutoff limit) suitable for H-mode confinement regime. The X2+X3 EC power available for the experiments studied here was 2.5 MW. The maximal NB power was up to 1.05 MW (including 15-20% of losses in the beam duct), using the tangentially injected beam with full energy of 25 keV at maximal power. Compared to the past, when fully non-inductive plasmas sustained using EC waves only were obtained, the operating space of advanced tokamak scenarios in TCV has been now extended towards higher plasma current and density with NB+EC heating scheme. These scenarios, characterized by high  $\beta_N$ , high non-inductive current

fraction and a relevant energetic particle (EP) population fraction ( $\sim 10\% n_e$ ) are envisaged as potential candidates for the regular future tokamak reactor operation due to their high fusion power generation and low inductive current requirements and outline the basis for future JT60-SA high- $\beta$  experimental program. An internal transport barrier can be generated by reversing the q-profile using EC current-drive (ECCD) [2]. A strong contribution of bulk ions and EP to plasma pressure and total energy in performed plasma discharges is illustrated in Figure 1: the plasma  $\beta$  (related to the plasma thermal content) is clearly decorrelated from electron thermal energy and this is caused by an interplay between neutral beam injection (NBI) and ECH.

**Indirect effects of EC** – EC waves are used to increase electron temperature and drive current, but this has some additional effects. In the discharges explored in this work, it causes a density pump-out which sums up with a high influx from the wall, causing both an increase of the plasma density, increase of neutral density (and charge-exchange (CX) EP losses) and increase of  $Z_{\text{eff}}$  (impurity density).  $Z_{\text{eff}}$  of  $\sim 3$  during EC&NB phases has been inferred (Figure 2) by computing the non-inductive contribution to plasma current [3,4]. This effect has been

<sup>♦</sup> See the author list "H. Meyer et al 2017 Nucl. Fusion 57 102014"

included for NBH modeling since the shielding of the EP current and the power deposition is affected by the impurities.

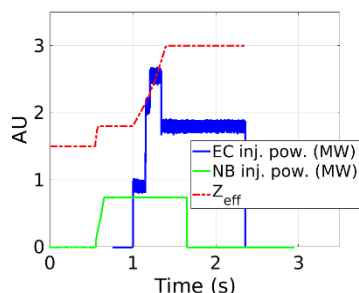


**Figure 2** – Example of  $Z_{\text{eff}}$  with varying auxiliary power

**Selection of plasma discharges** – Experimental sessions for developing high- $\beta_N$  and non-inductive scenarios explored several NBI and EC configurations. In this work, four discharges with co-current NBI have been selected; three 130 kA L-mode shots: on-axis NBI and co-current EC, off-axis NBI and co-current EC, off-axis NBI and counter-current EC and H-mode 150 kA on-axis NBI and co-current EC discharge. In all the cases,  $V_{\text{loop}}$  close to 0 indicates dominant non-inductive current drive.

**Modeling tools** – NUBEAM [5] and ASCOT [6] codes are used for NB EP modelling. NUBEAM is capable of a time-range interpretative simulation of the discharge, including CX EP losses. The code doesn't allow to compute orbits outside the separatrix (LCS). ASCOT is a full orbit solver allowing to calculate EP trajectories outside the LCS and to compute the EP loads on vessel walls. The interface of NUBEAM with TCV data has been done using OMFIT [7] suite and ASCOT simulation has been carried out for the first time in TCV.

**Power balance and current drive** – NB heating and CD characteristics vs EC injected power calculated by NUBEAM are shown in Figure 3. The absorbed power tends to decrease with increasing EC power (Fig. 3a). Orbit losses of EPs reaches  $\sim 20\%$  of NB injected power (Fig. 3b). CX EP losses increase with increasing EC power while the shine-through remains near constant. The non-inductive current grows with EC power, or at least remains constant. The decrease in shielding factor (computed as 1-shielded current/unshielded current) is linked to its dependence on  $Z_{\text{eff}}$  [8].

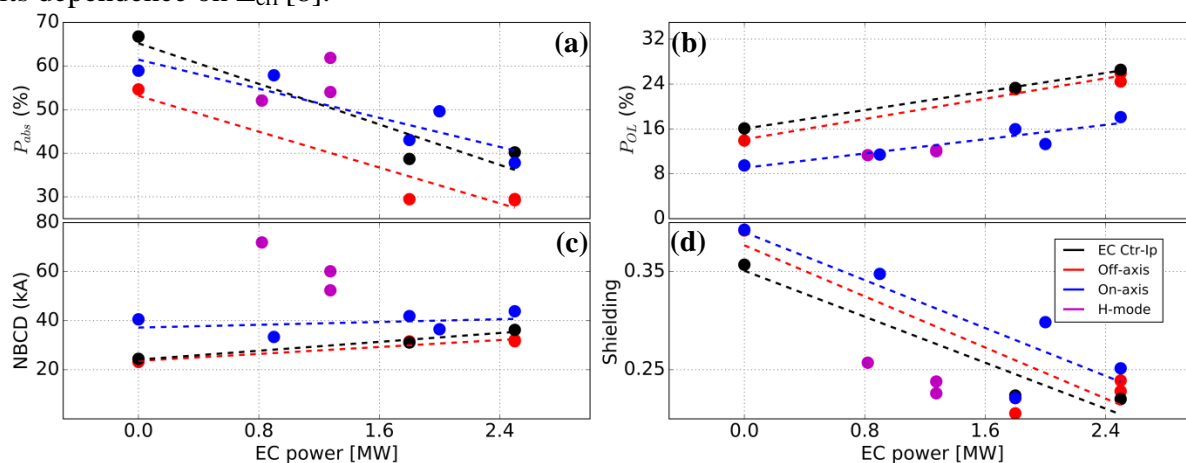


**Figure 3** NBH characteristics vs of EC power. (a) absorbed power (b) lost power (c) current drive (d) shielding. No trend plotted for H-mode due to the lack of points.

The EP slowing down power redistribution between ions and electrons is modified as well, in agreement with classical NB EP theory: the power fraction to ions increases by  $\sim 40\%$  at 2.5 MW of ECH, mostly due to change in  $T_e$ . The deposition profiles at maximal and zero EC power are shown in Figure 4. The pressure profiles (a) are broader and higher with ECH due to the density increase in the plasma outer region and related higher deposition of EP. The ratio of fast ion to electron density decrease (b) when injecting EC due to higher CX losses. The current drive (c) tends to decrease in the H-mode case, while in the other cases the profiles tend to be broader due to density increase at plasma low field side. This broadening of current density profile complicates the reversal of  $q$  profile needed for the sustainment of an internal transport barrier. Co- or counter- $I_p$  direction of EC injection has no effect on deposition profiles.

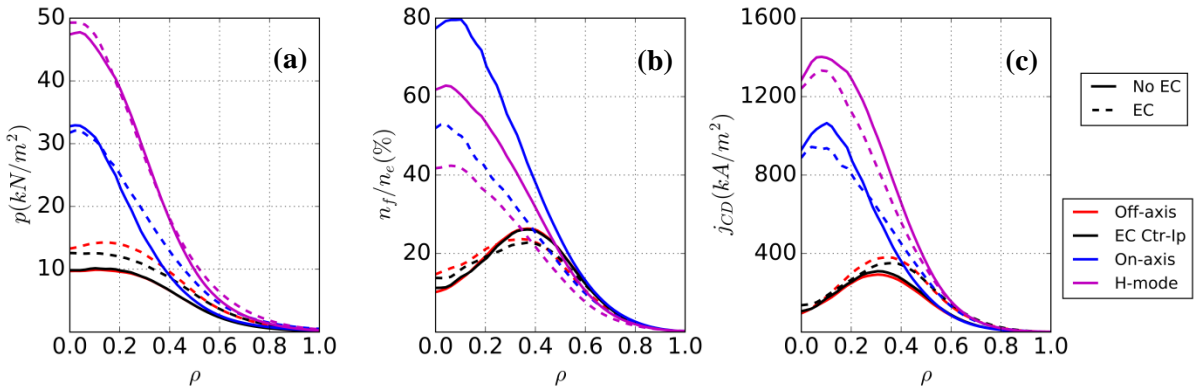


**Figure 4** NBH profiles (a) EP pressure (b) fraction of fast ions with respect to electron density (c) current density profile. Solid line: without ECH; dotted line: at maximum ECH power. The colors represent different shots.

**Fast ion distribution function** - The fast ion distribution function is strongly affected by ECH (Figure 5): energy distribution (a) is flatter with NBH only, while at the maximum EC power the peaks at NB full, half and 1/3 of injection energy (22.5 keV) are well pronounced. The EP energy distribution ( $\sim 1/E$ ) without ECH is typical for slowing-down without losses, but when EC power is added the slope of the curve tends to be positive, representing high EP losses (CX, orbit). Consequently, with NB only low-energy region ( $E < 6$  keV) are more populated. Furthermore, the increase of plasma temperature makes the particle collide mostly with ions and thus change preferentially their pitch ( $\xi = v_{\parallel}/v$ ) with respect to the energy. In Figure 5b we can note that the injection pitch (over 0.7) is less-populated when using EC power. Furthermore, adding EC power the population between  $0 < \xi < 0.7$  increases.

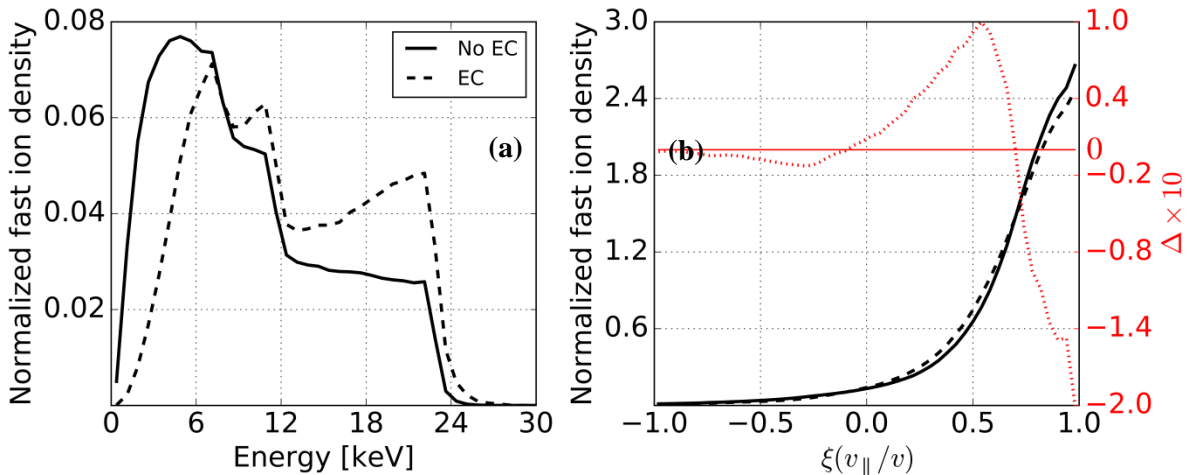


**Figure 5** Fast ion energy and pitch angle distributions as function of energy (a) and pitch (b). In (b) the difference between the two functions (no EC-max EC) is shown in red.

**EP wall loads** - Power deposition of EP to the TCV walls is calculated by ASCOT. In figure 6 the power loads to the wall are shown for the off-axis NB shot. The region where NBI EP born is indicated by black boxes. In both cases the losses are concentrated between  $-0.8$  rad and  $0.1$  rad (in poloidal angle  $\theta$ ), with a small contribution around  $\theta = -2$  rad (plasma leg of the X-point). Fig. 6 a-b show the first orbit losses with and without EC, where a peak at  $\varphi = 0$  (the opposite of the injection angle) can be seen. First orbit losses are slightly different adding EC power. Fig. 6 c-d show the total losses including EP transport (diffusion): adding EC power the maximum load scales of a factor of three, tends to be more concentrated on the midplane and spans a wider toroidal angle. The pitch-scattering collisions are stronger with EC, and particles enter orbits intersecting walls.

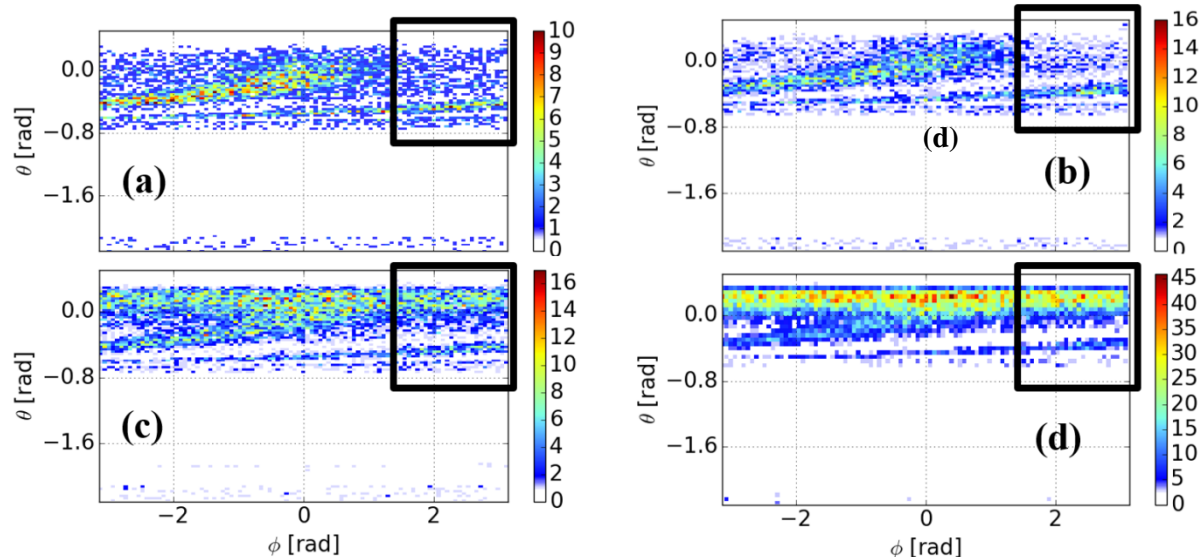


**Figure 6** EP losses to the wall. (a-b) - first orbit losses with and without EC respectively. (c-d) - total EP losses after the full slowing down with and without EC. The box shows the area where fast ions are born.

**Conclusions** – In this work, the nonlinear contribution of NBI on EC-heated TCV plasmas has been simulated. The results show that EC power injection interferes with NBI, increasing EP losses, and they must be confirmed by experimental data. The energy content of the plasma doesn't increase linearly with increasing additional power, due to the (indirect) interplay of many plasma processes: adding EC power  $Z_{\text{eff}}$  tends to increase and high influx from the wall makes the plasma density and neutral density to increase. NUBEAM simulations in OMFIT integrated framework show that the NBI plasma heating power decrease with the EC power injected. The current induced has a slight increase mostly due to the change in shielding factor (decreasing with increasing  $Z_{\text{eff}}$ ) and increase in density. H-mode plasma, on the other hand has opposite trends with L-mode plasmas. The EC waves injection influences also EP pressure and current drive profiles, which seems to increase (or at least move outwards), while the EP density decreases (remaining above 20% of electron density) due to increase of EP losses. Furthermore, the EP energy distribution changes adding EC power, making the injection energies more populated and the normalized density less spread. The slope of EP energy distribution changes from being negative (typical slowing-down distributions without losses) to being positive, representing strong losses. The  $v_{\parallel}/v = \xi > 0.7$  population tends also to decrease but the population with  $0 < \xi < 0.7$  increases, with the strongest difference for  $\xi \sim 1$ . ASCOT has been used for the first time on TCV and its simulations show that the particles are lost to the wall mostly on the outer mid-plane (high-field side-born particles), at about 180 deg from the injection position (hotter spot around  $\phi=0$ ). Adding EC, the losses concentrated even more on the outer mid-plane, reducing the toroidal asymmetry seen without EC. Our plans involve a deeper analysis of H-mode plasmas, which could be interesting due to higher absorbed power (and tendency to increase with EC power). The results of these simulations will be benchmarked with experimental data.

**Acknowledgment** This work has been carried out within the framework of the EUROfusion Consortium and has received funding from the Euratom research and training programme 2014-2018 under grant agreement No 633053. The views and opinions expressed herein do not necessarily reflect those of the European Commission.

- |   |   |
|---|---|
| [1] A.N.Karpushov, et al., FED <b>123</b> (2017)                    | [2] T. P. Goodman et al., PPCF <b>47</b> (2005)                             |
| [3] O. Sauter et al, Phys. Plasmas <b>1999</b>                      | [4] O. Sauter et al, Phys. Plasmas <b>2002</b>                              |
| [5] R. Goldston et al., J. of comput. phys. <b>43</b> (1981)        | [6] E. Hirvijoki et al., Comput. Phys. Commun. <b>185</b> (2014)            |
| [7] Meneghini, O., et al., Nuclear Fusion <b>55</b> (2015): 083008. | [8] Mikkelsen, D et al. Nuclear Technology-Fusion <b>4</b> (1983): 237-252. |